Australian Government
Department of Defence
Defence Science and
Technology Organisation

DSTO

# Ballistic and Material Testing Procedures and Test Results for Composite Samples for the TIGER Helicopter Vulnerability Project

A.D. Resnyansky and
G. Katselis

DSTO-TR-1617

Australian Government
Department of Defence
Defence Science and
Technology Organisation

# Ballistic and Material Testing Procedures and Test Results for Composite Samples for the TIGER Helicopter Vulnerability Project

*A.D. Resnyansky and G.Katselis*

**Weapons Systems Division**
Systems Sciences Laboratory

DSTO-TR-1617

**ABSTRACT**

The report describes procedures established for ballistic and material testing of composite samples in relation to the project on Battle Damage Repair and Vulnerability Studies (support to AIR87). Material tests of the samples involve measurements of the strength properties with Split Hopkinson Pressure Bar. The device designed and built up in WSD is briefly described. The report summarises the protocol and principal results of the ballistic and material tests.

*Published by*

*DSTO Systems Sciences Laboratory*
*PO Box 1500*
*Edinburgh South Australia 5111 Australia*

*Telephone: (08) 8259 5555*
*Fax: (08) 8259 6567*


*AR-013-192*
*September 2004*

**APPROVED FOR PUBLIC RELEASE**

# Ballistic and Material Testing Procedures and Test Results for Composite Samples for the TIGER Helicopter Vulnerability Project

## Executive Summary

The AIR87 project supports the introduction into service of Armed Reconnaissance Helicopters (ARH) and DSTO is taking part in Operational Tests and Evaluation of the ARH. As a part of the project, Weapons Systems Division (WSD) conducted development of procedures and preliminary tests on the ballistic damage of helicopter skin made from composite materials. The protocol development and tests have been conducted within a project covering the Battle Damage Repair issues for the Helicopter in operational conditions. The report describes procedures used for testing graphite epoxy composite samples and procedures employed for the impact velocity variations, fixture of samples and collection of results. The results are summarised as a set of impact and residual velocities, the difference between these is critical for the vulnerability of helicopter components and crew shielded by the skin. More detailed analysis of the issues related to energy absorption at impact along with implementation of an appropriate material model in the LS-DYNA3D hydrocode has been published in the 20th International Symposium on Ballistics [1]. Constitutive models involved in the hydrocode modelling of the high-velocity impact against a composite target require material properties at high strain rates. Such data can be obtained with an apparatus called Split Hopkinson Pressure Bar (SHPB). A SHPB capable of testing composites has been designed and built in WSD and it is briefly described in the report. Preliminary tests with the SHPB included calibration of the device and testing of conventional and composite materials. The tests confirmed the credibility of the device and the data obtained have been used in the constitutive model employed in [1]. Processing of the results and the development of penetration equations suitable for use in vulnerability codes has been published in the 21st International Symposium on Ballistics [2]. Structural analysis of the post-impact samples, which have been obtained in the present tests, as well as an ultra-sound inspection (C-scanning) of those has been published by J. Wang and R. Bartholomeusz [3]. The objective of the present report is to describe these procedures and methods in order and their application for conducting the ballistic and material tests on ARH composites and for analysis of the results [1-3].

1. Resnyansky, A.D. and Katselis, G., 2002. "Oblique Ballistic Impact Of Carbon Fibre Composite", *20th Int. Symp. on Ballistics*, 23-27 September 2002, Orlando, USA, Proceedings, v. II, 949-956.

2. Resnyansky, A.D. and Katselis, G., 2004. "Penetration Equations For Normal And Oblique Impact of Small Arms Projectiles Against Carbon-Fibre Composite Targets", *21st Int. Symp. on Ballistics,* 19-23 April 2004, Adelaide, Australia, CD-ROM Proceedings.

3. Wang, J. and Bartholomeusz, R., 2004. "Ballistic Damage In Carbon/Epoxy Composite Panels", *Journal of Battlefield Technology,* 7(1): 7-13.

# Authors

**Anatoly D. Resnyansky**
Weapons Systems Division

*Anatoly Resnyansky obtained a MSc in Applied Mathematics and Mechanics from the Novosibirsk State University (Russia) in 1979. In 1979-1995 he worked in the Lavrentyev Institute of Hydrodynamics (Russian Academy of Science) in the area of constitutive modelling for the problems of high-velocity impact. Anatoly obtained a PhD in Physics and Mathematics from the Institute in 1985. He joined the Weapons Effects group in 1998 where his current research interest include constitutive modelling and material characterisation at high strain rates, and theoretical and experimental analysis of physical processes involved in the weapon effects.*

**George Katselis**
Weapons Systems Division

*George Katselis obtained a BAppSci in Applied Physics from the Royal Melbourne Institute of Technology (RMIT) in 1992. He also completed a Ma(Eng) with the Microelectronic Materials and Technology Centre (MMTC) at RMIT in 1995. In 1995-1997 George was employed as a research assistant for Ceramic Fuel Cells Limited where he worked on high temperature oxidation resistant coatings before commencing at DSTO. He is currently working in the Weapons Effects group where he is developing sensors and instrumentation for measurement of blast and fragmentation effects of warheads. He is also involved in the design and evaluation of novel ordnance.*

# Contents

# 1. Introduction

The battle damage repair (BDR) program, associated with the ARH introduction, requires an assessment of damage and residual strength of the helicopter structures subject to small arms projectile impact. The structures of interest for the assessment are secondary structures like composite outer skins. The objective of the ballistic protocol is to describe a procedure for obtaining samples damaged under controlled impact conditions. An additional purpose of the vulnerability assessment (VA) is to estimate the energy absorbed by the samples during the impact. This energy can be an important factor for obtaining a correlation of the energy absorption results with measurements of residual strength in the CAI (compression after impact) and SAI (shear after impact) tests.

The residual velocity of the projectile is an important factor for vulnerability assessment of the threat to the structure and/or crew behind the outer skin of the helicopter. The energy absorbed by the skin is also related to the velocity drop associated with the difference between the impact velocity and the residual velocity of the projectile after the perforation.

To understand the nature of the target damage and derive physically based penetration equations for VA, a hydrocode simulation, predicting the response of the material to high-velocity impact, can be useful. To correctly model the impact response of composite samples a rate-sensitive constitutive model is required. Such a model [4], employed for the hydrocode simulation [1], needs strain-rate sensitive material properties of the composite material. The simulation can improve the understanding of the material response of the anisotropic materials such as composites, affecting the residual velocity especially at oblique impact.

In the present study, the projectile damaging the helicopter skin during the ballistic impact is a bullet launched by a small arms weapon. Testing of coupons made from carbon-epoxy composite material was conducted. Conventional rifled weapons utilising 5.56x45 mm, 7.62x51 mm, and 12.7x99 mm cartridges were used. The material properties have been obtained with a Split Hopkinson Pressure Bar (SHPB) that has been used for testing of the composite samples of 13x13x8 mm dimensions with the quasi-isotropic layout.

# 2. Experimental Set-Up for the Ballistic Tests

## 2.1 Sample Fixture and Dimensions

Results of ballistic tests available in the literature suggest that the damage of a composite sample at high-velocity impact is localised within a zone close to the area of impact. Keeping in mind the moderate size of the projectiles and the thicknesses of the target, the time duration of the penetration process (for impact velocities ranging between 300 and 1200 m/s) is in the order of 10-50 μsec. With the velocity of shear waves in the target being in the order of 2 mm/μsec, the impact effect extends over a linear distance of

approximately 3-10 cm. Therefore, sample dimensions with side length of 10 cm were considered to be reasonable.

If α denotes the angle between the line of fire and a normal to the target surface (the incidence or the obliquity angle), then the actual aim-spot at oblique impact increases by $1/\sin(\alpha)$ compared with the normal incidence. This factor should be taken into account when determining the sample dimensions. The localised damage area increases in the same proportion, but the effect of impact due to propagation of the shear waves is nearly the same as with a frontal impact. Therefore, the size of the sample in the relevant direction for oblique impact was enlarged (although, not proportionally to $1/\sin(\alpha)$).

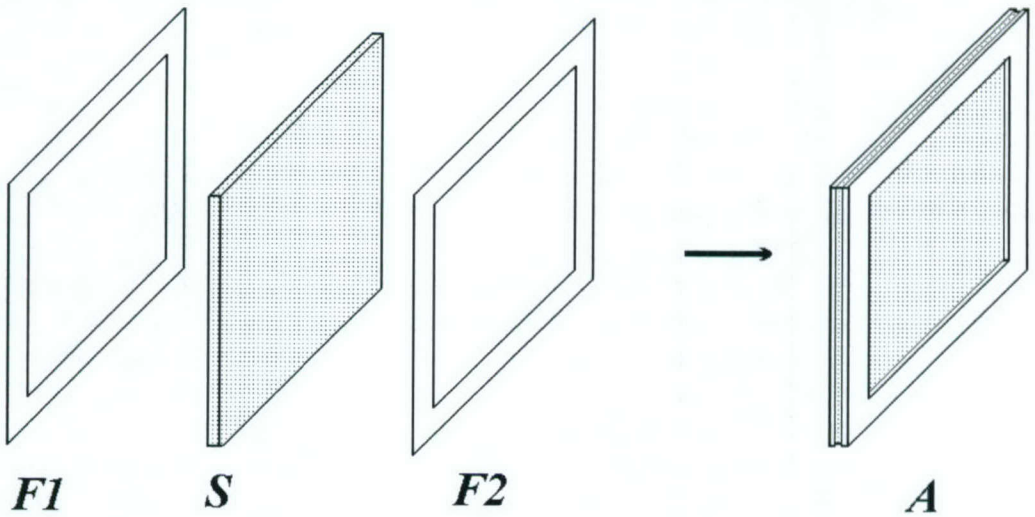


*Figure 1. Assembly of the sample set-up. F1 and F2 - frames, S - sample (coupon), A - completed assembly (bolted).*

The assembly procedure of the sample set-up is shown in Fig. 1. Sample *S* is placed between two rigid steel frames (*F1* and *F2*) and clamped around the sample's perimeter by M6 socket head bolts. The sample *S* has width *W*, length *L*, and thickness *T* (see Fig. 2 (a)). The width was the same for all tests for the vulnerability assessment and this was 100 mm. The length is chosen depending on the incidence of bullet impact. For ballistic tests with the obliquity angle larger than 45° the length *L* is chosen to be 150 mm, for smaller obliquity angles the length is coincident with the width and it is 100 mm.

For ballistic tests of samples prepared for the CAI/SAI tests, the samples are of slightly different dimensions but still cover the minimum impact affected zone selected above. For the CAI tests the coupons are of the same configuration with *W*=*L*=274 mm. For coupons used in the SAI tests, the frame is supposed to be of larger dimensions than that for the VA tests (*LxW* is approximately 250x250 mm) and the configuration of the frame bolts was aligned with the internal holes (six around each side) manufactured for the SAI testing machine (Fig. 2(b)).

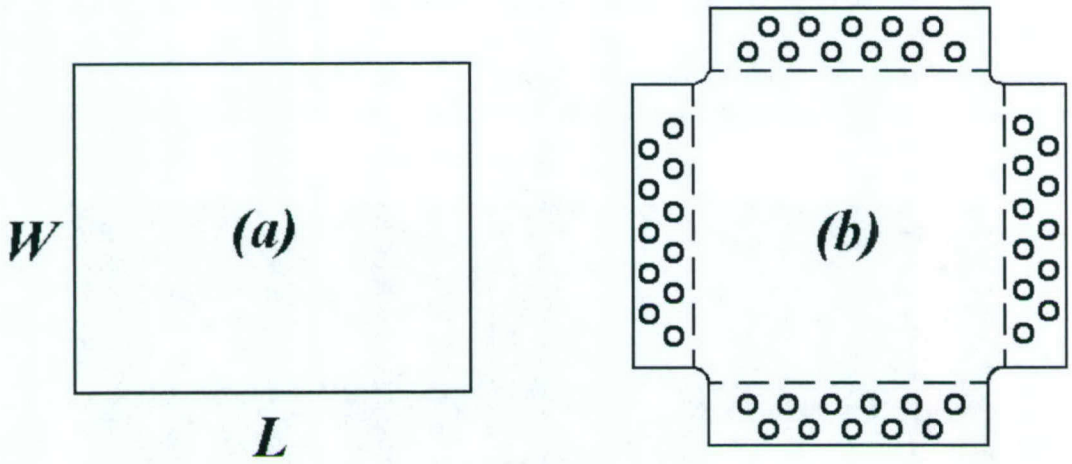


*Figure 2. Samples used for the ballistic testing. (a) - schematic of a sample for the vulnerability assessment and for the CAI tests; (b) – a sample for the SAI tests.*

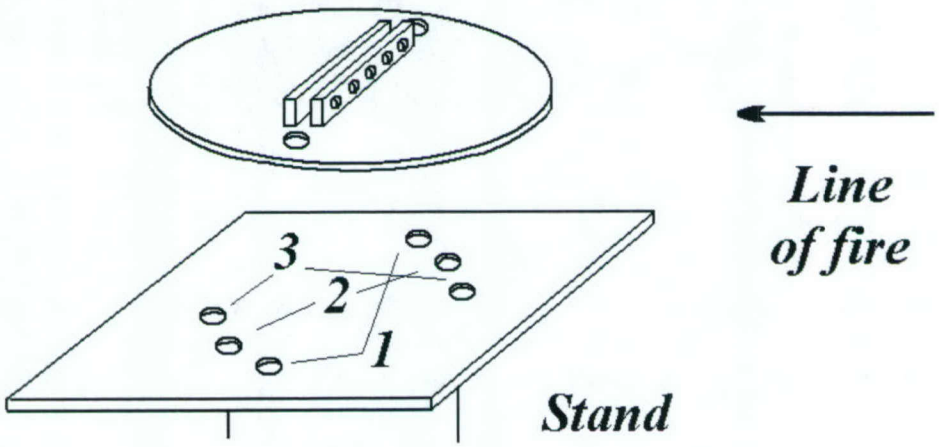


*Figure 3. Schematic of the fixture used for the sample set-up. The sample fixture (disc at the top) is pinned into the position 1 for the zero obliquity angle, into 2 - for the 30° obliquity angle, and into 3 - for the 60° obliquity angle.*

The sample set-up described in Fig. 1 is then mounted (bolted) into a sample fixture, which is a disc that can be rotated and pinned into three positions on the target stand (Fig. 3). The positions were varied to achieve the three obliquity angles required by the BDR program specifications of 0, 30 and 60 degrees respectively.

In summary, the mounting of the samples using this arrangement was as follows:

- selected sample is mounted in a suitable frame (three possible options: i) the vulnerability assessment; ii) the CAI tests; and iii) the SAI tests). This is then assembled into the sample set-up;
- the sample set-up is bolted into the rotating disc sample fixture;
- the sample fixture is mounted onto the target stand according to the required obliquity angle.

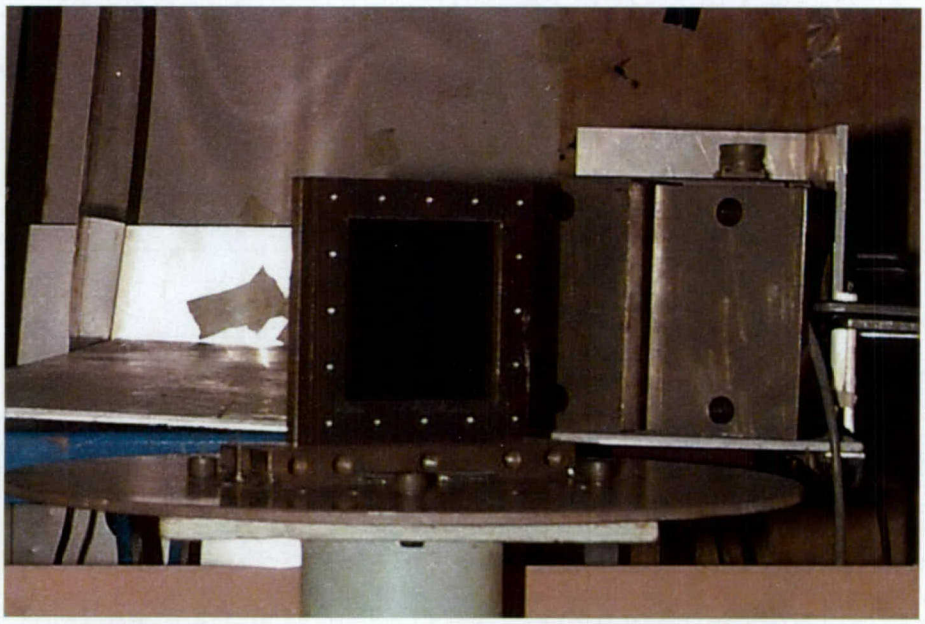

*Figure 4. Photograph of the fixture used for the sample set-up (front view for the 30° obliquity angle set-up).*

The entire sample fixture was covered by thin plastic sheeting (for occupational health and safety reasons) in order to contain dispersion of the composite target debris. The subsequent assembly was positioned in the firing range as described in the following section.

Several Aluminium and GLARE coupons have also been tested against the ballistic threat. The same sample dimensions at normal and oblique impact conditions have been employed and the same method of clamping has been applied. Four GLARE coupons with a thickness of 1.5 mm have been tested. The GLARE material [5] consists of 2 layers of Aluminium with the epoxy layer in between. Projectile calibres used for the testing of the GLARE coupons were 5.56 and 7.62 mm.

## 2.2 Firing Range Set-up

Basic elements of the current firing range configuration include the sample set-up described in the above section, a firing unit (a rifled weapon of the calibre required) and two chronographs (one in front of the target and one directly behind the target) (Fig. 5).

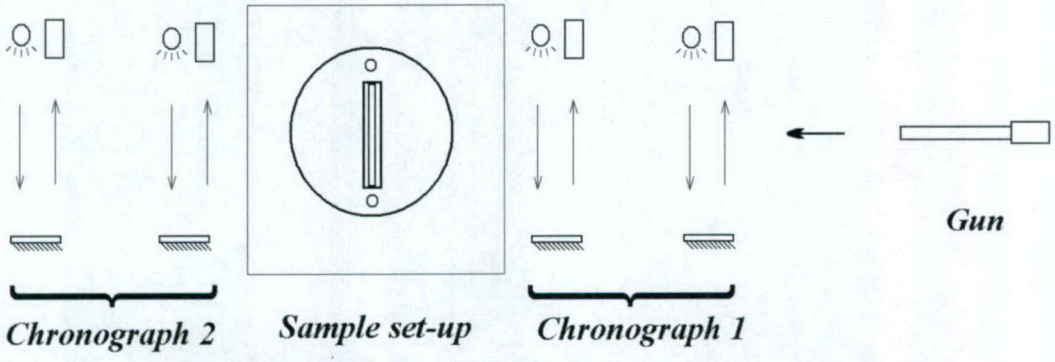


*Figure 5. Layout of the firing range set-up.*

The sketched gun shown in Fig. 5 consists of a stationary gun mount with replaceable barrel and breech unit. In the current test program the following calibres were used: 5.56, 7.62 and 12.7 mm. All projectiles were of the full metal jacket (FMJ) or ball variety. The 12.7 mm-calibre set-up is shown in Fig. 6.

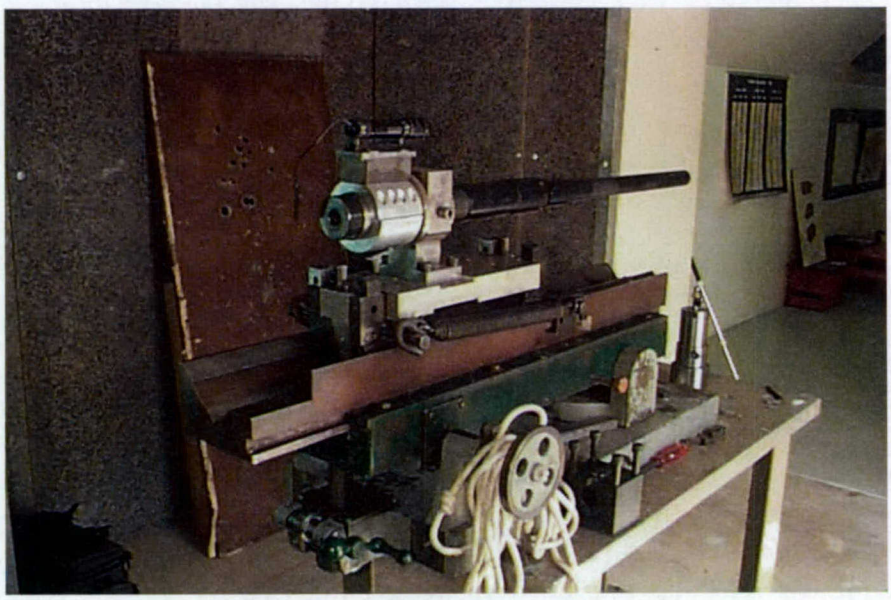

*Figure 6. Photograph of the firing unit (gun) in the working position*

The current indoor ballistic range set-up is limited to the use of ball ammunition (not tracer or incendiary types) and is also limited to the velocity range that can be achieved by varying the propellant charge weights and the cartridge volume. The screens of each of the chronographs are spaced 1m apart. The rear chronograph (corresponding to chronograph 2 in Fig. 5) set-up is shown in Fig. 7.

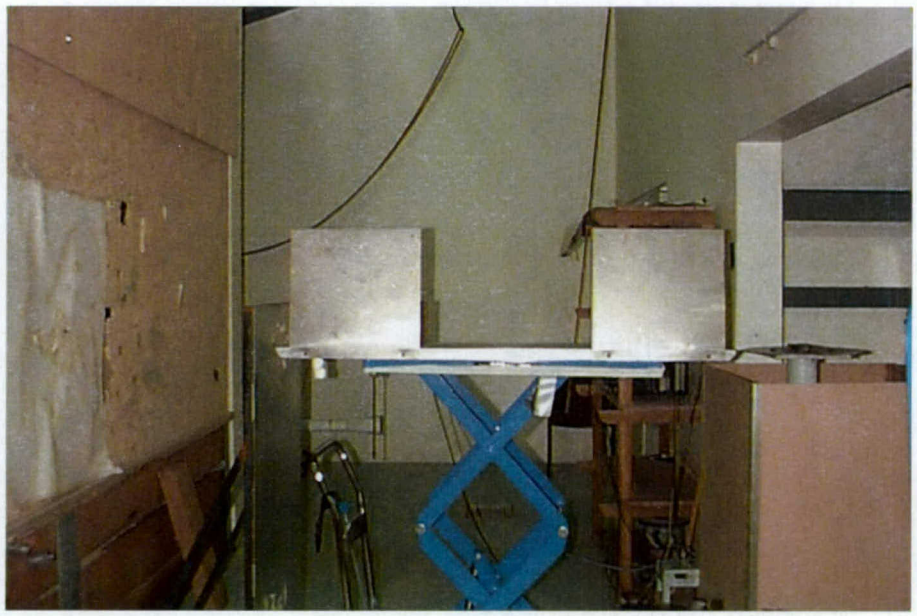

*Figure 7. Photograph of the rear chronograph (chronograph 2 in Fig. 5) with the target stand shown on the right hand side (view from the mirrors' side).*

# 3. Ballistic Test Results

As stated earlier, the bullet types used were standard military ball projectiles. Typical projectile weights were approximately 62 grains for the 5.56 mm-calibre weapon, 144 grains for the 7.62mm-calibre, and 645 grains for the 12.7 mm-calibre. To achieve a variety of velocities for the vulnerability assessment data, different propellant charge weights and propellant types were used. Standard military ball ammunition was used for reaching maximum velocity in the tests. The average velocities for these were: 975 m/s for the 5.56x45 mm, 880 m/s for the 7.62x54 mm and 900 m/s for the 12.7x99 mm cartridges. More precise data on the initial velocity $V_i$ was recorded with chronograph 1 (see schematic in Fig. 5) and listed in the table below, which summarises the results of the test firings. For lower velocities the following reduced charge weights were used for the 5.56 mm-cartridges:

- 6 grains of HER2400 - expected velocity of 350 m/s
- 7 grains of AR2205 - expected velocity of 360 m/s
- 8.5 grains of AR2205 - expected velocity of 470 m/s
- 9.5 grains of Blue Dot - expected velocity of 620 m/s;

for the 7.62 mm-cartridges:

- 9.5 grains of HER2400 - expected velocity of 310 m/s
- 11.5 grains of AR4201 - expected velocity of 390 m/s
- 12 grains of AR4201 - expected velocity of 400 m/s

- 23 grains of AR2205 - expected velocity of 630 m/s;

and for the 12.7 mm-cartridges:

- 62 grains of AR2206 - expected velocity of 450 m/s.

Here HER signifies the HERCULES brand of propellant, while AR2205, AR2206, and AR4201 are propellants manufactured by ADI (Australian Defence Industries). It should be noted that a modified case with a reduced internal volume was used to reduce velocity of 12.7 mm-projectiles.

The ballistic data of the 59 shots that were undertaken are summarised in Table 3.1. The Table states the projectile calibre *C*, the sample thickness *T*, type of material (the composite is marked as CF – Carbon Fibre), the obliquity angle $\alpha$, the impact velocity $V_i$ measured with the first chronograph of schematic in Fig. 5, the residual velocity $V_r$ measured with the second chronograph, and an evaluation of the ballistic limit velocity $V_{50}$ conducted with formulas published in [2]. Traditionally, $V_{50}$ is the impact velocity at which the target perforation occurs with the probability of 50%. The penetration equation involving $V_{50}$ and the details associated with calculation of $V_{50}$ are also discussed in [2].

*Table 3.1 Results of Ballistic Tests*

| SHOT # | C | T | Material | $\alpha$ | $V_i$ | $V_r$ | $V_{50}$ |
|---|---|---|---|---|---|---|---|
| 1 | 5.56 | 5.0 | AL | 0 | 379.03 | 284.58 | 250.36 |
| 2 | 5.56 | 5.0 | AL | 0 | 974.75 | 943.84 | 243.52 |
| 3 | 5.56 | 1.5 | CF | 0 | 356.85 | 350.34 | 67.85 |
| 4 | 5.56 | 3.0 | CF | 0 | 337.64 | 320.93 | 104.90 |
| 5 | 5.56 | 4.5 | CF | 0 | 330.96 | 298.77 | 142.38 |
| 6 | 5.56 | 4.5 | CF | 0 | 460.98 | 432.30 | 160.06 |
| 7 | 5.56 | 6.0 | CF | 0 | 360.17 | 304.72 | 192.01 |
| 8 | 5.56 | 6.0 | CF | 0 | 621.43 | 589.69 | 196.06 |
| 9 | 5.56 | 6.0 | CF | 0 | 976.75 | 949.31 | 229.89 |
| 10 | 5.56 | 1.5 | CF | 30 | 340.07 | 331.94 | 73.92 |
| 11 | 5.56 | 3.0 | CF | 30 | 974.09 | 954.56 | 194.08 |
| 12 | 5.56 | 1.5 | CF | 60 | 359.47 | 354.17 | 61.50 |
| 13 | 5.56 | 1.5 | GLARE | 30 | 336.04 | 302.85 | 145.62 |
| 14 | 7.62 | 5.0 | AL | 0 | 882.07 | 848.03 | 242.68 |
| 15 | 7.62 | 1.5 | CF | 0 | 281.81 | 271.96 | 73.86 |
| 16 | 7.62 | 1.5 | CF | 0 | 414.97 | 406.62 | 82.83 |
| 17 | 7.62 | 1.5 | CF | 0 | 633.31 | 628.02 | 81.68 |
| 18 | 7.62 | 3.0 | CF | 0 | 295.31 | 269.74 | 120.20 |
| 19 | 7.62 | 3.0 | CF | 0 | 632.99 | 622.24 | 116.16 |
| 20 | 7.62 | 3.0 | CF | 0 | 881.91 | 865.35 | 170.10 |
| 21 | 7.62 | 3.0 | CF | 0 | 894.53 | 879.20 | 164.90 |
| 22 | 7.62 | 4.5 | CF | 0 | 284.01 | 235.43 | 158.85 |
| 23 | 7.62 | 4.5 | CF | 0 | 391.25 | 369.37 | 129.01 |
| 24 | 7.62 | 4.5 | CF | 0 | 886.76 | 860.73 | 213.28 |
| 25 | 7.62 | 6.0 | CF | 0 | 319.54 | 245.34 | 204.73 |

| | | | | | | | |
|---|---|---|---|---|---|---|---|
| 26 | 7.62 | 6.0 | CF | 0 | 627.04 | 600.82 | 179.43 |
| 27 | 7.62 | 6.0 | CF | 0 | 870.32 | 846.38 | 202.73 |
| 28 | 7.62 | 1.5 | GLARE | 0 | 329.60 | 314.12 | 99.82 |
| 29 | 7.62 | 1.5 | CF | 30 | 399.36 | 393.52 | 68.05 |
| 30 | 7.62 | 3.0 | CF | 30 | 392.91 | 384.39 | 81.38 |
| 31 | 7.62 | 3.0 | CF | 30 | 638.73 | 630.99 | 99.13 |
| 32 | 7.62 | 3.0 | CF | 30 | 876.58 | 865.05 | 141.71 |
| 33 | 7.62 | 4.5 | CF | 30 | 392.43 | 371.29 | 127.06 |
| 34 | 7.62 | 6.0 | CF | 30 | 393.38 | 348.83 | 181.84 |
| 35 | 7.62 | 1.5 | GLARE | 30 | 402.19 | 394.76 | 76.95 |
| 36 | 7.62 | 1.5 | CF | 60 | 382.76 | 379.29 | 51.42 |
| 37 | 7.62 | 1.5 | CF | 60 | 885.35 | 874.81 | 136.21 |
| 38 | 7.62 | 1.5 | CF | 60 | 531.38 | 520.94 | 104.82 |
| 39 | 7.62 | 3.0 | CF | 60 | 395.29 | 380.53 | 107.01 |
| 40 | 7.62 | 3.0 | CF | 60 | 870.40 | 853.24 | 171.98 |
| 41 | 7.62 | 3.0 | CF | 60 | 886.05 | 876.12 | 132.28 |
| 42 | 7.62 | 4.5 | CF | 60 | 384.79 | 337.04 | 186.65 |
| 43 | 7.62 | 4.5 | CF | 60 | 875.35 | 847.89 | 217.53 |
| 44 | 7.62 | 6.0 | CF | 60 | 391.93 | 274.55 | 279.70 |
| 45 | 7.62 | 6.0 | CF | 60 | 865.05 | 824.95 | 260.32 |
| 46 | 7.62 | 1.5 | GLARE | 60 | 371.91 | 339.97 | 150.79 |
| 47 | 12.7 | 5.0 | AL | 0 | 910.41 | 892.62 | 179.10 |
| 48 | 12.7 | 1.5 | CF | 0 | 905.96 | 904.98 | 42.13 |
| 49 | 12.7 | 3.0 | CF | 0 | 438.33 | 430.00 | 85.05 |
| 50 | 12.7 | 3.0 | CF | 0 | 907.69 | 904.81 | 72.25 |
| 51 | 12.7 | 4.5 | CF | 0 | 456.33 | 448.37 | 84.86 |
| 52 | 12.7 | 4.5 | CF | 0 | 898.55 | 892.22 | 106.47 |
| 53 | 12.7 | 6.0 | CF | 0 | 449.52 | 437.03 | 105.23 |
| 54 | 12.7 | 6.0 | CF | 0 | 909.26 | 897.99 | 142.72 |
| 55 | 12.7 | 3.0 | CF | 30 | 901.23 | 898.88 | 65.04 |
| 56 | 12.7 | 1.5 | CF | 60 | 455.81 | 453.17 | 48.99 |
| 57 | 12.7 | 1.5 | CF | 60 | 883.63 | 881.52 | 61.03 |
| 58 | 12.7 | 3.0 | CF | 60 | 437.33 | 431.09 | 73.61 |
| 59 | 12.7 | 3.0 | CF | 60 | 912.57 | 906.45 | 105.51 |

# 4. Split Hopkinson Pressure Bar Tests

## 4.1 The SHPB Set-Up

The Split Hopkinson Pressure Bar (SHPB) is used for measurement of yield stress of materials at high strain rate conditions [6]. The schematic of the measurement device is shown in Fig. 8.

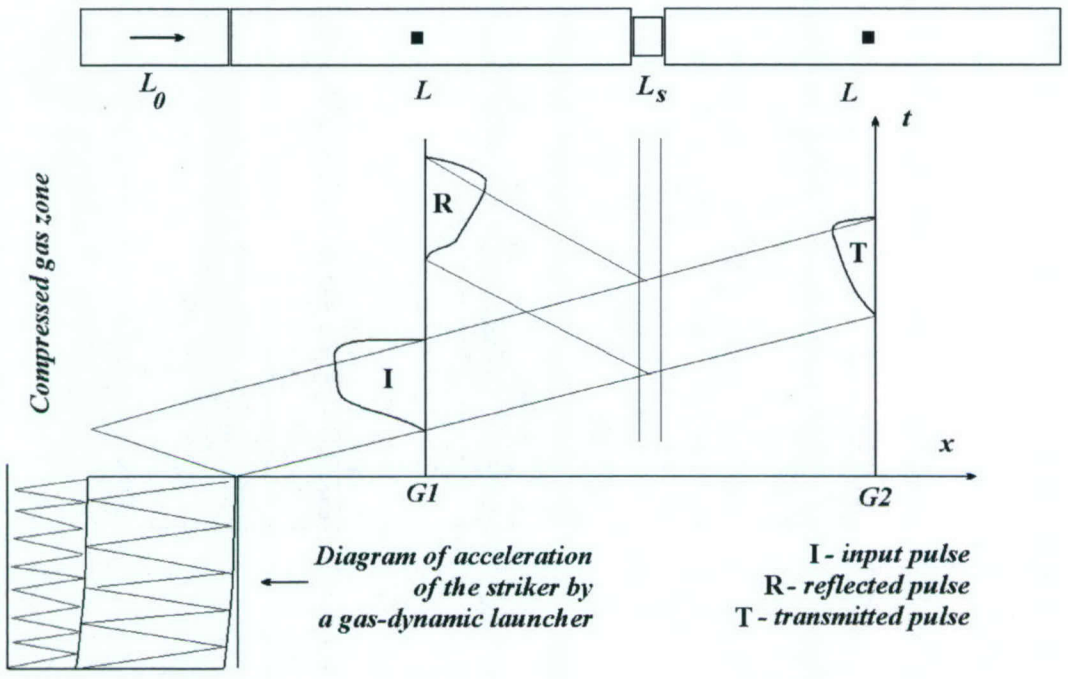


*Figure 8. Schematic of the Split Hopkinson Pressure Bar. $L_0$ is the striker bar, L – the incident (left) and transmitting (right) bars. $L_s$ –sample.*

Gauges *G1* and *G2*, which are mounted at the centre of the input (incident) and output (transmitter) bars, are recording the strain pulses (pulses *I* and *R* in Fig. 8 by the input bar gauge and *T* – by the output bar gauge). These records inform us about the stress-strain response of the sample and the strain rate at which the bar is loaded [6]. When compressed, a sample is exposed to plastic deformation conditions, whereas the bar elements of the device, made of maraging steel, are under elastic deformation conditions, because the ratio of the bar diameter to that of the sample is selected to be less than 1. Therefore, the bar diameter is critical for testing composite materials because the structural features of the material sample tested should be essentially less than the sample diameter. Thus, the use of miniaturised SHPBs, which are presently very popular, is limited for the testing of composites.

The necessary length-to-diameter ratio [6] of the bars dictates relatively long input and output rods of the SHPB device. The device, which we designed and installed in the WSD material testing laboratory, is shown in Fig. 9. It consists of two 2 m-length and 2 cm-diameter input and output rods mounted on a heavy I-beam base. The firing unit is mounted on a separate stand in order to avoid transmitting the shot vibration to the gauges. The firing unit is operated remotely and utilizes commercial (Ramset) propellant cartridges allowing us to employ a variety of striker rod lengths (from 10 up to 30 cm in length).

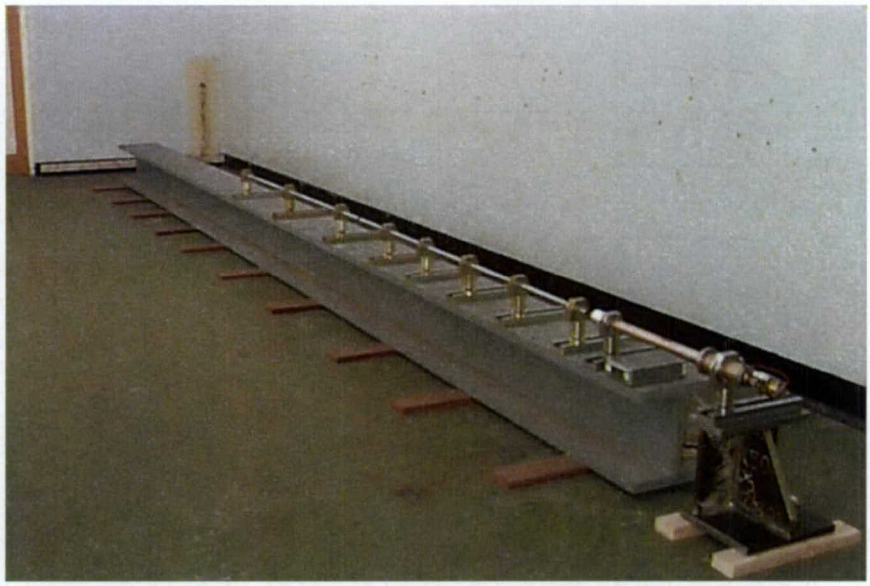

*Figure 9. General view of the SHPB designed and employed in WSD for testing composite samples*

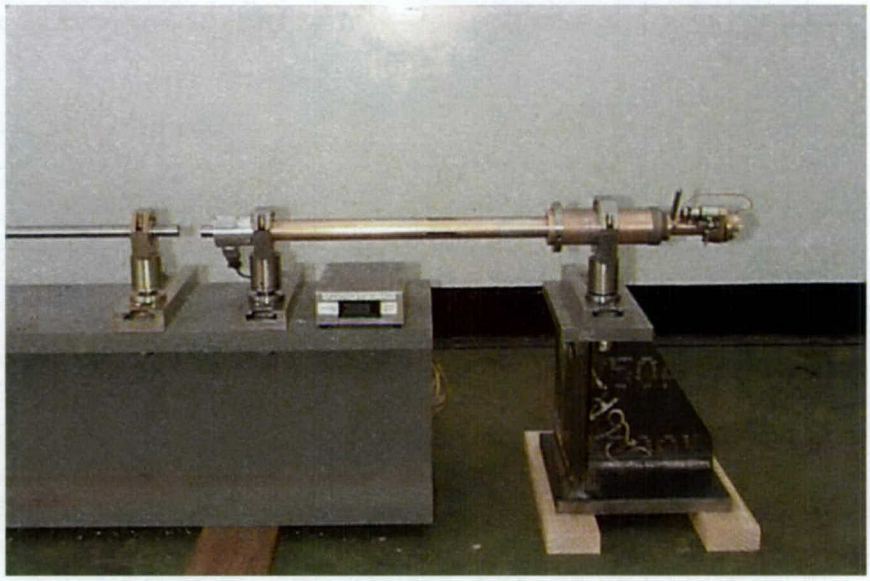

*Figure 10. General view of the firing unit. The unit is detached from the main components of the SHPB. The firing is managed by a miniature motor operated from outside. The velocity of the striker bar is measured with optical sensors and displayed on the electronic readout located below the barrel.*

The firing unit is shown in detail in Fig. 10. It consists of a long barrel with slots for releasing the pressurised gas after propellant ignition. The striker bar is separated from the breach chamber by spacers of variable length in order to allow for a variation of the impactor velocity (by varying the expansion volume). Different strengths of cartridges are also used for the same purpose. The velocity range for the impactor is from 10 up to

30 m/s. This velocity is recorded with an electronic unit based on the optical sensors. The actual surface of the end of the striker bar impacting the input bar is slightly rounded to allow for smearing-off of the front of the stress pulse.

The resulting data are recorded with a TDS-744 oscilloscope with signals via two Tektronix ADA400A differential pre-amplifiers.

## 4.2 The Test Results

The stress pulses have been calculated using 1-wave, and, occasionally 2-, and 3-wave analyses [6]. In the simplest case, when using the 1-wave analysis, the pulse *R* (Fig. 8) is employed for calculation of strain rate and the pulse *T* is used for calculation of stress. The device has been calibrated without a sample adjusting the stress pulses with the signal voltage assuming the maraging steel properties are known (supplier data have been used).

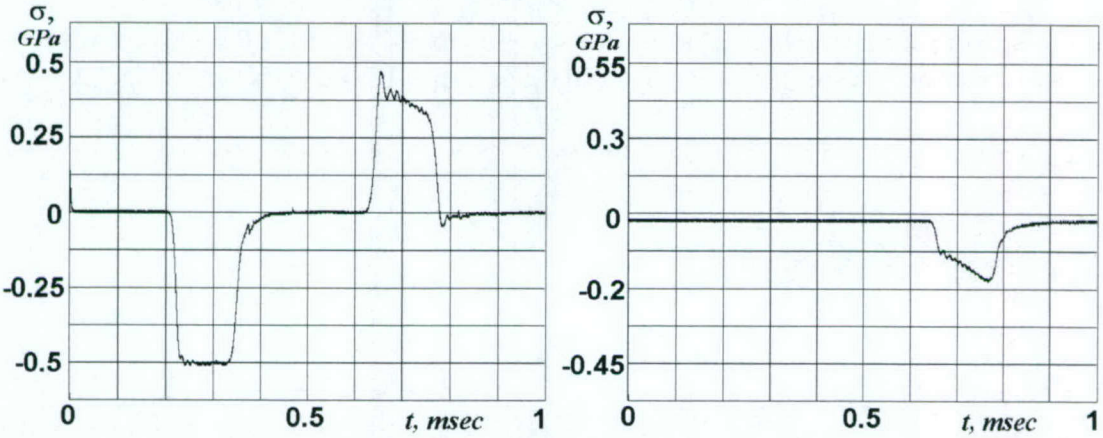


*Figure 11. Data from gauges G1 (left plot) and G2 (right plot) for a copper sample at the striker bar velocity of 22.4 m/s.*

We assumed that the Young modulus $E$=210 GPa, the steel density is $\rho$=7.85 g/cm$^3$, and the elastic wave velocity $c$ in the rods is calculated as follows $c=(E/\rho)^{1/2}$. Then, using the velocity $u$ behind the front pulse as $u=V_0/2$, where $V_0$ is the velocity of the striker bar, the stress $\sigma$ for the calibration purposes was calculated as $\sigma = \rho\, c\, u$. The calibration resulted in the correspondence of 240 mV to 0.1 GPa=100 MPa.

The data has been verified with copper samples. The stress pulses from the gauges *G1* and *G2* (Fig. 8) are shown in Fig. 11. The impactor velocity in the present case is $V_0$=22.4 m/s. The voltage has been replaced by appropriate stress from the results of calibration. The OFHP copper samples were of cylindrical shape with a height of 5 mm and 10 mm in diameter.

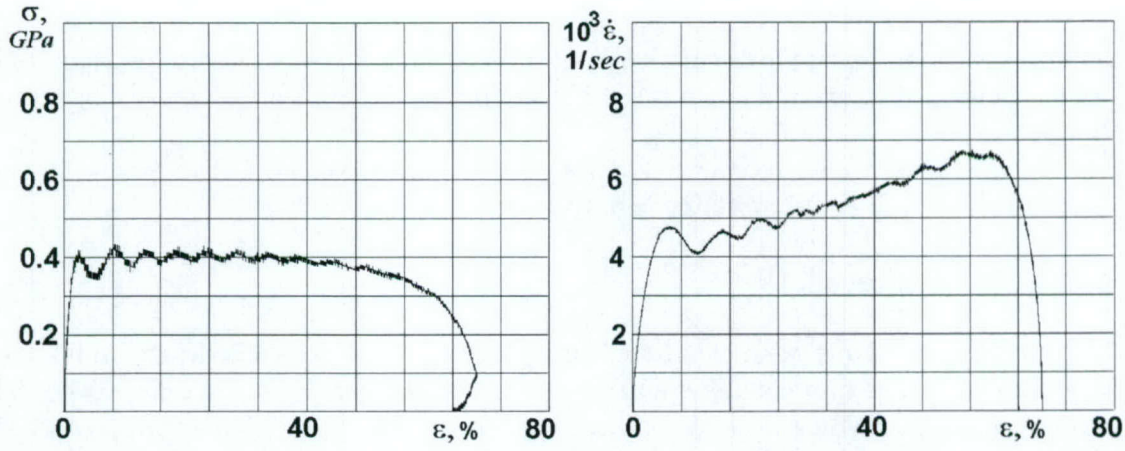


*Figure 12. Stress versus strain (left plot) and strain rate versus strain (right plot) obtained with 1-wave analysis of the strain pulses for the copper sample.*

The result of processing the pulses with 1-wave analysis, shown in Fig. 11, gives the stress versus strain and strain-rate versus strain diagrams, which are shown in Fig. 12.

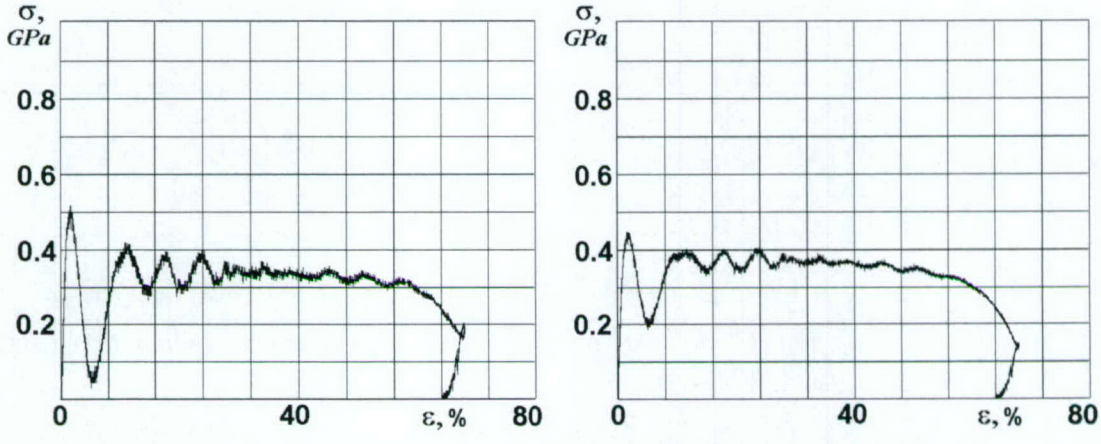


*Figure 13. SHPB analyses (stress versus strain) of the test of Fig. 11 for the copper sample: 2-wave analysis (left plot) and 3-wave analysis (right plot).*

The yield stress is slightly less than that published in [7], probably, due to the fact that the strain rate in the tests [7] is essentially lower than the one achieved in the present tests. Comparison of the present results with experiments published in [8-9] on the testing of copper in similar conditions demonstrates very good agreement.

The results of 2- and 3-wave analyses shown in Fig. 13 demonstrate low frequency oscillations associated with the non-equilibrium at the initial stage of loading, which is discussed in detail in [10-11]. Specifically, the Pochhammer-Chree oscillations and non-ideality of the loading stress pulse (a deviation from the Π-shape) may result in a slight divergence of the yield stress level between the 1- and 2-wave analyses for hardening material that was noted in [9, 11].

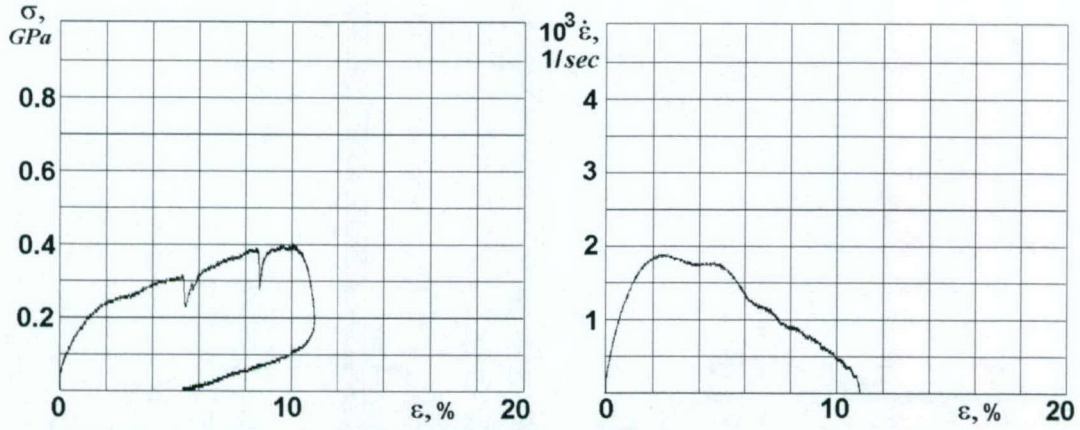


*Figure 14. Stress versus strain (left plot) and strain rate versus strain (right plot) obtained with 1-wave analysis of the strain pulses for a composite sample. The striker bar velocity is 14 m/s.*

The result in Fig. 14 was obtained with the SHPB testing of a composite sample of 13x13x8 mm in dimensions and an impactor velocity of 14 m/s. The composite sample was of the quasi-isotropic layout (20 plies in the wave propagation direction with thickness in this direction of 8mm); this layout provides nearly orthotropic isotropy of the material in the direction of loading. The dips in the stress-strain response, shown in Fig. 14, possibly result from a delamination when loading the material.

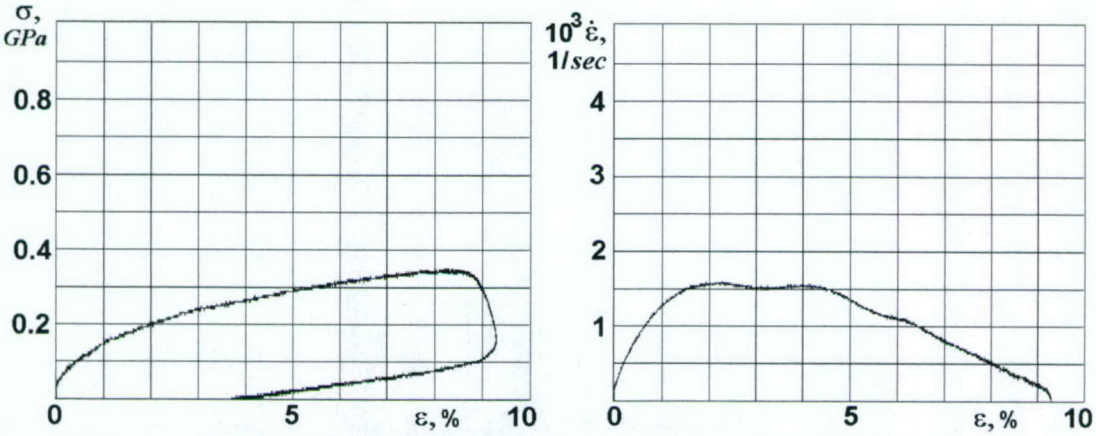


*Figure 15. Stress versus strain (left plot) and strain rate versus strain (right plot) obtained with 1-wave analysis of the strain pulses for a composite sample. The striker bar velocity is 12 m/s.*

Fig. 15 describes similar results for a test of a composite sample of the same dimensions at the impactor velocity of 12 m/s. The inverse branch of the stress-strain response, which is associated with unloading of the sample after the compression, is typical for the SHPB tests and it does not characterize material properties. Strain rate level at the second test is slightly less than previously (1500 $sec^{-1}$ instead of nearly 1800 $sec^{-1}$ in the previous test) but allows us to observe some rate dependence of the stress response.

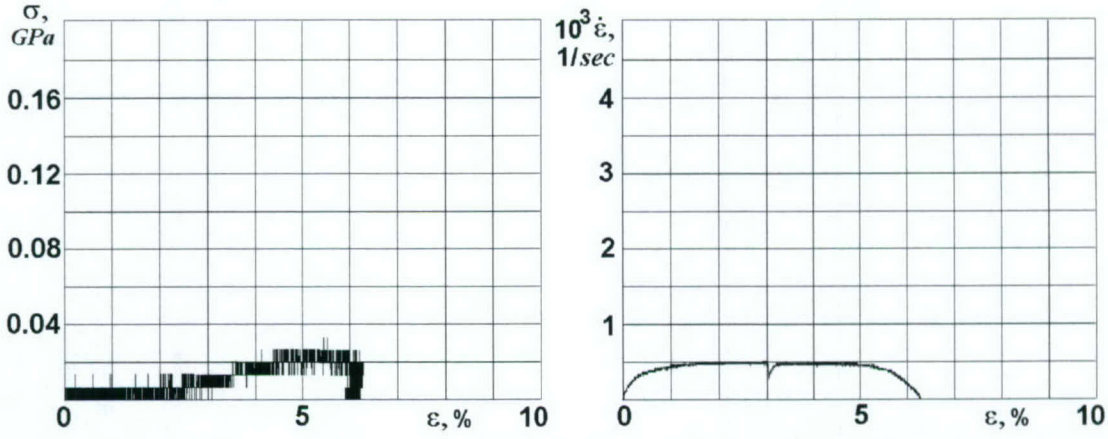


*Figure 16. Stress versus strain (left plot) and strain rate versus strain (right plot) obtained with 1-wave analysis of the strain pulses for a composite sample. The striker bar velocity is 4 m/s.*

For completeness we describe a low strain rate result obtained at the impactor velocity of approximately 4 m/s (Fig. 16). An unusually low stress response could be associated with several factors: voltage resolution of oscilloscope has been set up for a higher impact velocity (this is seen as a non-smooth stress strain diagram in Fig. 16); extensive delamination during longer time of loading might be present; and the adhesive epoxy has a high rate sensitivity (this is partly confirmed, for example, by SHPB data for epoxy published in [7]).

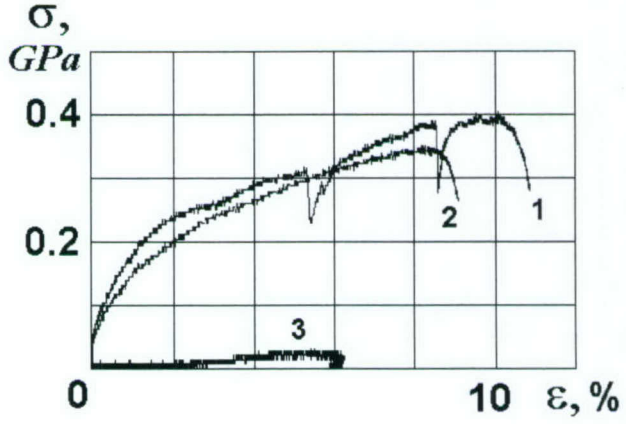


*Figure 17. Summary of the tests on the stress-strain response for the carbon fibre composite at three strain rates: 1 – 1800 sec$^{-1}$; 2 – 1500 sec$^{-1}$; and 3 – 500 sec$^{-1}$*

The results of the tests for the carbon fibre composite are summarised in Fig. 17. Strain-rate sensitivity is observed. However, repeating similar tests would be useful for confirmation of the rate sensitivity of the material stress limit. Reference [12] on the tensile stress limit of a carbon fibre composite confirms a high-rate sensitivity and the present level of yield

stress observed. In addition, reference [13] confirms the stress level of 400MPa for compression tests with a SHPB for a graphite epoxy composite, not supporting, however, the fact of very high rate sensitivity of the material.

# 5. Conclusion

Testing procedures have been developed for conducting ballistic tests of composite samples within the BDR program. An experimental facility suitable for SHPB testing of composite samples has been designed and built as a part of the WSD material testing laboratory.

An experimental program has been realised for assessment of the ballistic and material properties of helicopter skin materials. The preliminary SHPB results have been used for validation of a constitutive model and hydrocode results. The ballistic tests have been employed for derivation of analytical penetration equations that are needed for vulnerability assessment.

# 6. Acknowledgement

The composite samples were supplied by R. Bartholomeusz and L. Mirabella of Air Vehicles Division. The GLARE samples were provided by Mr. John Rowe of Aviation Equipment Australia Pty, Ltd. The authors are grateful to Eddie Almond, Jeff Ackers and Shaun McCormack of WSD for their help in conducting the ballistic tests.

# 7. References

1. Resnyansky, A.D. and Katselis, G., 2002. "Oblique Ballistic Impact Of Carbon Fibre Composite", 20th Int. Symp. on Ballistics, 23-27 September 2002, Orlando, USA, Proceedings, v. II, 949-956.
2. Resnyansky, A.D. and Katselis, G., 2004. "Penetration Equations For Normal And Oblique Impact of Small Arms Projectiles Against Carbon-Fibre Composite Targets", 21st Int. Symp. on Ballistics, 19-23 April 2004, Adelaide, Australia, CD-ROM Proceedings.
3. Wang, J. and Bartholomeusz, R., 2004. "Ballistic Damage In Carbon/Epoxy Composite Panels", *Journal of Battlefield Technology*, 7(1): 7-13.
4. Resnyansky, A.D. and Romensky, E.I., 1997. "Using a Homogenization Procedure for Prediction of Material Properties and the Impact Response of Unidirectional Composite", 11th Int. Conf. on Composite Materials, Gold Coast, Queensland, Australia,

14-18 July 1997, Proceedings, Vol. II: Fatigue, Fracture and Ceramic Matrix Composites, (Ed. Murray L. Scott), Australian Composite Structures Society, Woodhead Publishing Ltd, pp. 552-561.

5. Hughes, D., 2004. "'Glare' factory ramps up", *Aviation Week & Space Technology*, 160(14): 66-67.

6. Gray III, G.T., 2000. "Classic Split-Hopkinson Pressure Bar Technique", Mechanical Testing and Evaluation, ASM - Handbook, Volume 8 (Kuhn, H. and Medlin, D., eds.), Metals Park, OH, ASM International, pp. 462-476.

7. Lindholm, U.S., 1964. "Some Experiments With The Split Hopkinson Pressure Bar", *J. Mech. Phys. Sol*, 12: 317-335.

8. Nemat-Nasser, S., Isaacs J.B., and Starrett J.E., 1991. "Hopkinson Techniques For Dynamic Recovery Experiments", *Proc. R. Soc. Lond. A.*, 435: 371-391.

9. Follansbee, P.S. and Frantz, C., 1983. "Wave Propagation in the Split Sopkinson Pressure Bar", *J. Eng. Materials Techn.*, 105: 61-66.

10. Resnyansky, A.D., 2000. "Study of Influence of Loading Method on Results of the Split Hopkinson Bar", Structural Failure and Plasticity, IMPLAST 2000, Proc the 7th Int. Symp. on Structural Failure and Plasticity, 4-6 October 2000, Melbourne, Australia, pp. 597-602.

11. Resnyansky, A.D. and Gray III, G.T., 2003. "Numerical Simulations of the Influence of Loading Pulse Shape on SHPB Measurements", CP620, Shock Compression of Condensed Matter - 2001, American Institute of Physics, pp. 315-318.

12. Liu, Z.G. and Chiem, C.V., 1988. "A New Technique for Tensile Testing of Composite Materials at High Strain Rates", *Experimental Techniques*, 12(3): 20-21.

13. Dee, A.T., Vinson, J.R., and Leon, G., 1997. "High Strain Rate Mechanical Properties of a Torospherical Shell Composed of IM7/E7T1-2 Graphite Epoxy Composite", 11th Int. Conf. on Composite Materials, Gold Coast, Queensland, Australia, 14-18 July 1997, Proceedings, Vol. V: Textile Composites and Characterisation, (Ed. Murray L. Scott), Australian Composite Structures Society, Woodhead Publishing Ltd, pp. 693-703.

DISTRIBUTION LIST

Ballistic and Material Testing Procedures and Test Results for Composite Samples for the TIGER Helicopter Vulnerability Project

A.D. Resnyansky and G.Katselis

**AUSTRALIA**

**DEFENCE ORGANISATION**

| | **No. of copies** |
|---|---|
| **S&T Program** | |
| Chief Defence Scientist<br>FAS Science Policy<br>AS Science Corporate Management<br>Director General Science Policy Development | shared copy |
| Counsellor Defence Science, London | Doc Data Sheet |
| Counsellor Defence Science, Washington | Doc Data Sheet |
| Scientific Adviser to MRDC, Thailand | Doc Data Sheet |
| Scientific Adviser Joint | 1 |
| Navy Scientific Adviser | Doc Data Sht & Dist List |
| Scientific Adviser – Army | Doc Data Sht & Dist List |
| Air Force Scientific Adviser | Doc Data Sht & Dist List |
| Scientific Adviser to the DMO M&A | Doc Data Sht & Dist List |
| Scientific Adviser to the DMO ELL | Doc Data Sht & Dist List |
| **Systems Sciences Laboratory** | |
| Chief of Weapons Systems Division | Doc Data Sht & Dist List |
| Research Leaders: | |
| Dr. N. Burman | 1 |
| Dr. N. Martin | 1 |
| Head of the Weapons Effects Group: John Waschl | 1 |
| Author(s): | |
| Dr. A. Resnyansky | 1 |
| George Katselis | 1 |
| Dr. A.E. Wildegger-Gaissmaier | 1 |
| DSTO, SPD, Russell Offices, Russell Drive<br>Canberra, ACT 2600 | |
| **Air Vehicles Division** | |
| Richard Bartholomeusz | 1 |
| DSTO, AVD, 506 Lorimer St, Fishermans Bend VIC 3207 | |
| **DSTO Library and Archives** | |
| Library Edinburgh | 1 + Doc Data Sheet |
| Defence Archives | 1 |
| **Capability Systems Division** | |
| Director General Maritime Development | Doc Data Sheet |
| Director General Information Capability Development | Doc Data Sheet |
| **Office of the Chief Information Officer** | |
| Deputy CIO | Doc Data Sheet |

Director General Information Policy and Plans — Doc Data Sheet
AS Information Strategies and Futures — Doc Data Sheet
AS Information Architecture and Management — Doc Data Sheet
Director General Australian Defence Simulation Office — Doc Data Sheet

**Strategy Group**

Director General Military Strategy — Doc Data Sheet
Director General Preparedness — Doc Data Sheet

**Navy**

Director General Navy Capability, Performance and Plans, Navy Headquarters
Doc Data Sheet
Director General Navy Strategic Policy and Futures, Navy Headquarters
Doc Data Sheet

**Air Force**

SO (Science) - Headquarters Air Combat Group, RAAF Base, Williamtown NSW 2314 — Doc Data Sht & Exec Summ
WOFF Don McLean — 1
CAMM2 Project Office
139 Canberra Ave
Fyshwick ACT 2609

**Army**

ABCA National Standardisation Officer, Land Warfare Development Sector, Puckapunyal — e-mailed Doc Data Sheet
SO (Science), Deployable Joint Force Headquarters (DJFHQ) (L), Enoggera QLD — Doc Data Sheet
SO (Science) - Land Headquarters (LHQ), Victoria Barracks NSW — Doc Data & Exec Summ
MAJ Christopher Kassulke — 1
Bldg 45, Army Aviation Systems Program Office
Orrs Road Oakey QLD 4401

**Intelligence Program**

DGSTA Defence Intelligence Organisation — 1
Manager, Information Centre, Defence Intelligence Organisation — 1 PDF
Assistant Secretary Corporate, Defence Imagery and Geospatial Organisation
Doc Data Sheet

**Defence Materiel Organisation**

Deputy CEO — Doc Data Sheet
Head Aerospace Systems Division — Doc Data Sheet
Head Maritime Systems Division — Doc Data Sheet
Chief Joint Logistics Command — Doc Data Sheet
Head Materiel Finance — Doc Data Sheet
Head Materiel Finance — Doc Data Sheet

**Defence Libraries**

Library Manager, DLS-Canberra — Doc Data Sheet
Library Manager, DLS - Sydney West — Doc Data Sheet

**OTHER ORGANISATIONS**

National Library of Australia — 1
NASA (Canberra) — 1

John W. Rowe, — 1
Aviation Equipment Australia Pty Ltd,
301/20 Gerrale St., Cronulla NSW 2230

**UNIVERSITIES AND COLLEGES**

Australian Defence Force Academy
Library — 1
Head of Aerospace and Mechanical Engineering — 1
Serials Section (M list), Deakin University Library, Geelong, VIC — 1
Hargrave Library, Monash University — Doc Data Sheet
Librarian, Flinders University — 1

**OUTSIDE AUSTRALIA**

**INTERNATIONAL DEFENCE INFORMATION CENTRES**

US Defense Technical Information Center — 2
UK Dstl Knowledge Services — 2
Canada Defence Research Directorate R&D Knowledge & Information Management (DRDKIM) — 1
NZ Defence Information Centre — 1

**ABSTRACTING AND INFORMATION ORGANISATIONS**

Library, Chemical Abstracts Reference Service — 1
Engineering Societies Library, US — 1
Materials Information, Cambridge Scientific Abstracts, US — 1
Documents Librarian, The Center for Research Libraries, US — 1

Alexis Boccard, — 1
Eurocopter – France,
13725 Marignane Cedex, FRANCE

Gérard Loroit, — 1
DGA/CEAT, Materials and Structures Division
23, Avenue Henri Guillaumet
31056 Toulouse Cedex, FRANCE

Patrick Sancho — 1
DGA/CEAT, Structures and Fire Protection Division
23, Avenue Henri Guillaumet
31056 Toulouse Cedex, FRANCE

Oliver Peppin — 1
MINDEF/DGA (TER),
26, boulevard Victor 00457 Armées
Paris, FRANCE

| | |
|---|---|
| Bruno Hilaire<br>DGA/CTA<br>16 bis, Avenue Prieur de la Côte d'Or<br>94114 ARCUEIL Cedex France | 1 |
| Michel Gimonet,<br>DGA/ETBS -Etablissement Technique de Bourges<br>Rocade Est, Echangeur de Guerry<br>18021 Bourges Cedex | 1 |
| SPARES | 5 |
| **Total number of copies: 42 Printed + 1 pdf =** | **43** |

**DEFENCE SCIENCE AND TECHNOLOGY ORGANISATION**
**DOCUMENT CONTROL DATA**

1. PRIVACY MARKING/CAVEAT (OF DOCUMENT)

2. TITLE

Ballistic and Material Testing Procedures and Test Results for Composite Samples for the TIGER Helicopter Vulnerability Project

3. SECURITY CLASSIFICATION (FOR UNCLASSIFIED REPORTS THAT ARE LIMITED RELEASE USE (L) NEXT TO DOCUMENT CLASSIFICATION)

| | |
|---|---|
| Document | (U) |
| Title | (U) |
| Abstract | (U) |

4. AUTHOR(S)

A.D. Resnyansky and G.Katselis

5. CORPORATE AUTHOR

Systems Sciences Laboratory
PO Box 1500
Edinburgh South Australia 5111 Australia

| 6a. DSTO NUMBER | 6b. AR NUMBER | 6c. TYPE OF REPORT | 7. DOCUMENT DATE |
|---|---|---|---|
| DSTO-TR-1617 | AR-013-192 | Technical Note | September 2004 |

| 8. FILE NUMBER | 9. TASK NUMBER | 10. TASK SPONSOR | 11. NO. OF PAGES | 12. NO. OF REFERENCES |
|---|---|---|---|---|
| 2004/1067705 | LRR 04/122 | DSTO | 16 | 13 |

13. URL on the World Wide Web

http://www.dsto.defence.gov.au/corporate/reports/DSTO-TR-1617.pdf

14. RELEASE AUTHORITY

Chief, Weapons Systems Division

15. SECONDARY RELEASE STATEMENT OF THIS DOCUMENT

*Approved for public release*

OVERSEAS ENQUIRIES OUTSIDE STATED LIMITATIONS SHOULD BE REFERRED THROUGH DOCUMENT EXCHANGE, PO BOX 1500, EDINBURGH, SA 5111

16. DELIBERATE ANNOUNCEMENT

No Limitations

17. CITATION IN OTHER DOCUMENTS Yes

18. DEFTEST DESCRIPTORS

High Velocity, Vulnerability, Damage assessment, Weapons effects, Materials, Helicopter performance

19. ABSTRACT

The report describes procedures established for ballistic and material testing of composite samples in relation to the project on Battle Damage Repair and Vulnerability Studies (support to AIR87). Material tests of the samples involve measurements of the strength properties with Split Hopkinson Pressure Bar. The device designed and built up in WSD is briefly described. The report summarises the protocol and principal results of the ballistic and material tests.